Tomographic Q Estimation for Viscoacoustic Imaging

A. Valenciano* (PGS) & N. Chemingui (PGS)

SUMMARY

Viscoacoustic imaging in anisotropic media is achieved by tomographic estimation of the earth attenuation (Q model), and prestack wave equation migration. The proposed Q tomography algorithm uses spectral ratios computed on surface seismic data as the input. An integral tomographic equation relates the Q model with the measured spectral ratios. The tomography numerical implementation results in a linear inversion scheme that we solve by conjugate gradient methods with 3D regularization. The output Q model is combined with VTI or TTI anisotropic models to perform model-driven attenuation and anisotropy compensation during imaging. To that effect we use a viscoacoustic anisotropic Fourier finite differences one-way wave equation migration. Results from a synthetic example and a VTI field dataset from the North Sea demonstrate the accuracy of our tomographic estimation of Q, and the effectiveness of the viscoacoustic wave equation migration for attenuation compensation.

Introduction

Seismic waves are attenuated as they travel through the subsurface of the earth. Attenuation causes a loss of high-frequency energy, and generally distorts the wavelet's phase (dispersion). Seismic attenuation and dispersion are usually compensated for in the time domain during data conditioning and preprocessing. A simple attenuation model, described by the quality factor (Q), is used in practice.

This simple assumption is not accurate if the Q model varies rapidly. Waves arriving at different offsets follow ray paths that sense different attenuation profiles e.g., shallow hydrates in the Gulf of Mexico, gas chimneys in the North Sea, etc. (Chen and Huang, 2010; Yu et al., 2002). Under these conditions estimating the Q model using a tomographic approach (Brzostowski and McMechan, 1992) is necessary. Later at the compensation step, the tomographic Q, combined with VTI or TTI anisotropic models, can be used to perform viscoacoustic wave-equation prestack depth migration (PSDM) that can handle the propagation complexity (Valenciano et al., 2011).

In this paper we present a workflow comprising a tomographic approach to derive interval Q models of the subsurface from surface seismic data, followed by attenuation compensation during viscoacoustic wave-equation prestack depth migration. The Q estimation uses spectral ratios for input data and a tomographic forward operator parameterized in the inverse of Q for modeling. The numerical inversion is performed using a conjugate gradient solver and Laplacian operator for regularization. The depth migration is based on a Fourier Finite Differences viscoacoustic one-way wave equation algorithm (Valenciano et al., 2011). The viscoacoustic migration effectively accounts for the effects of the attenuation anomalies on the amplitudes and kinematics of the final image. We demonstrate the accuracy of our solution on a synthetic example and a 3D VTI field dataset from the North Sea.

Theory: Q estimation and compensation

Brzostowski and McMechan (1992) adapted to exploration seismology a tomographic Q estimation formalism already in use by earthquake seismologists (Ho-Liu, 1989). It is based on the following equation:

$$-\frac{2}{\omega}\ln\left[\frac{A_k}{A_0}\right] = \int_{\text{ray}\,k} Q^{-1}(x,y,z)\, v^{-1}(x,y,z)\, ds \equiv t_k^*, \quad (1)$$

that relates the inverse of Q to measured spectral ratios.

In Equation (1), A_k are the seismic spectrum measured at a seismic horizon, A_o is a reference seismic spectrum measured at a horizon not affected by attenuation, ω is the radial frequency, v is the velocity model, Q is the quality factor, and t^* is the attenuated travel time. Given a dataset consisting of spectral estimates at various times, equation 1 provides a linear system in Q^{-1}.

Equation (1) was derived under the assumption that geometrical spreading, scattering, or other non Q-related factors have been removed from the data. It can be expressed in matrix form $\mathbf{d}=\mathbf{Fm}$ (Rickett, 2006), where $\mathbf{d}$ contains log-spectral estimates (A_k/A_0) at interpreted seismic horizons, $\mathbf{F}$ is a chain of linear operators consisting of a diagonal matrix (containing the frequencies) and a path integration operator, and $\mathbf{m}$ is the $Q^{-1}(x,y,z)$ model to estimate.

We pose an inversion problem to solve for the model that minimizes the least-squares objective function,

$$O = (\mathbf{d} - \mathbf{Fm})^{\mathrm{T}}(\mathbf{d} - \mathbf{Fm}) + \varepsilon\, \mathbf{m}^{\mathrm{T}}\nabla^{\mathrm{T}}\nabla\mathbf{m}, \quad (2)$$

which contains a regularization with a Laplacian operator ∇, and a balancing parameter ε.

After solving for an attenuation model, the Q compensation can be performed with a viscoacoustic Wave Equation Migration (WEM). Our solution is based on a Fourier Finite-Difference (FFD) scheme for migration by wavefield continuation (Valenciano et al., 2011). Similarly to the acoustic solution, the viscoacoustic migration consists of three terms: phase-shift extrapolation, thin-lens correction, and finite-differences correction. The viscoacoustic migration was also extended to account for anisotropy (VTI and TTI). The dispersion relation, in presence of attenuation, includes both real and imaginary terms. While the real part controls the kinematics of the image, the imaginary part recovers the high vertical wave numbers in the seismic image; therefore improving resolution and amplitude balance. The implementation is stable, efficient, and very flexible. In absence of attenuation or anisotropy, the solution reduces to the familiar isotropic acoustic case.

Synthetic data example

We generated a viscoacoustic dataset using a constant velocity model (2000 m/s) and a variable Q model shown in the top panel of Figure 2. The modeling code is based on solving the one-way viscoacoustic wave equation to derive an adjoint to the migration operator discussed in Valenciano et al. (2011).

The data consists of 350 shots spaced at 50 m, each with 500 channels with the offset ranging from zero to 6237.5 m. Three flat reflectors were modeled. Figure 1 shows the modeled data: zero offset section (top), and a time slice taken at 3.292 sec (bottom). Notice the decay in amplitudes and the phase change of the reflectors below the attenuation anomalies. Also notice the distortion to the AVO response by the V shape amplitude patterns in the midpoint-offset panel (Kjartansson, 1979).

Since the data were generated using one-way viscoacoustic wave equation modeling, there are no multiples, converted waves, or other propagation factors affecting the amplitudes. Thus we can assume that most amplitude effects that are not

related to attenuation have been removed from the data. This assumption can be challenging to satisfy when processing field data.

The logarithm of the spectral ratios for the top and bottom reflector is used as the input to the tomography. The frequency used ranged from 4 to 40 Hz). Different offsets provided complementary information, contributing in different ways to the tomographic result.

Figure 2 shows the tomographic result, the anomalies are resolved, since multiple offsets ranging from zero to 6000 m were used as input to the tomography. However, when processing field data the offset range is a trade off parameter. One have to take into account the practicality of using long offsets in the tomography. Far offset data are the most affected by wave propagation effects non-related to attenuation.

Field data from the North Sea

We applied the Q tomography and the migration with Q compensation to a 3D dataset from the North Sea. The data was acquired with dual-sensor streamers comprised of hydrophones and vertical geophones. The area is characterized by a gas chimney, which hampers the imaging of reflectors at the oil reservoir level, and by a significant VTI anisotropy. Therefore, a workflow that addresses both problems is necessary to image the reservoir.

We used our Q tomography to derive the attenuation model using offsets up to 4000 m. Figure 3 shows the 3D Q model, a low Q (high attenuation) anomaly is clearly resolved.

Later, we performed VTI wave equation migrations with and without the Q compensation (Valenciano et al., 2011). The resulting images spectrum comparison after depth to time conversion is shown in Figure 4. The Q compensated result shows a broader spectrum where amplitudes for high frequencies are enhanced.

In Figure 5 we compare a close up of the VTI migrations with and without the Q compensation. The Q compensation using the tomographic model greatly improves the continuity and resolution at the reservoir level. The latest is also corroborated by Figure 6, which shows a comparison of the RMS amplitude attribute without and with Q compensation. Note how the white "anomalous" area is greatly reduced as well as how the resolution of stratigraphic features is enhanced.

Conclusions

We presented a viscoacoutic-imaging workflow for tomographic estimation of Q models and attenuation compensation during depth migration.

The synthetic data results demonstrate that when tomographic modelling assumptions are met, the Q anomalies can be accurately estimated through multi-offset tomography.

Using field data form the North Sea, we showed that our Q tomography followed by VTI viscoacoustic wave equation depth migration greatly reduce the footprint of Q anomalies in the final images. Consequently enhancing the image of the reservoir.

Acknowledgements

References

Brzostowski M. A., and G. A. McMechan, 1992, 3D tomographic imaging of near-surface seismic velocity and attenuation: Geophysics, **57**, 396.

Chen, Y., and Y. Huang, 2010, Use Q-RTM to image beneath gas hydrates in Alaminos Canyon, Gulf of Mexico: 80th Annual International Meeting, SEG, Expanded Abstracts, 3165–3170.

Ho-Liu, P., Montagner, I.-P., and Kanamori, H., 1989, Comparison of iteractive back-projection inversion and generalized inversion without blocks: Case studies in attenuation tomography: Geophys. J., 97, 19-29.

Kjartansson E., 1979, Attenuation of seismic waves and applications in energy exploration: thesis, Stanford University.

Rickett J., 2006, Integrated estimation of interval-attenuation profiles: Geophysics, **71**, no. 4, A19–A23

Valenciano A. A., N. Chemingui, D. Whitmore, and S. Brandsberg-Dahl, 2011, Wave equation migration with attenuation and anisotropy compensation: 81st Annual International Meeting, SEG, Expanded Abstracts, **30**, 232.

Yu, Y., R. S. Lu, and M. M. Deal, 2002, Compensation for the effects of shallow gas attenuation with viscoacoustic wave-equation migration: 72nd Annual International Meeting, SEG, Expanded Abstracts, **21**, 2062-2065.
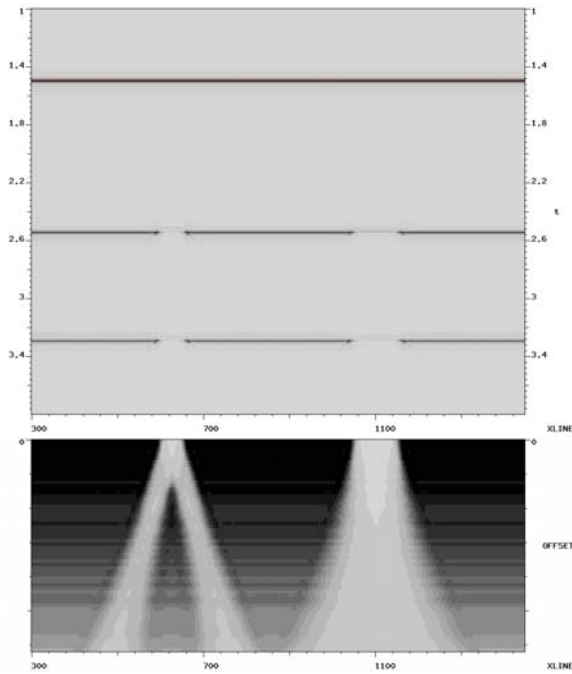
Figure 1 Model data: zero offset section (top), and time slice taken at 3.292 sec (bottom).
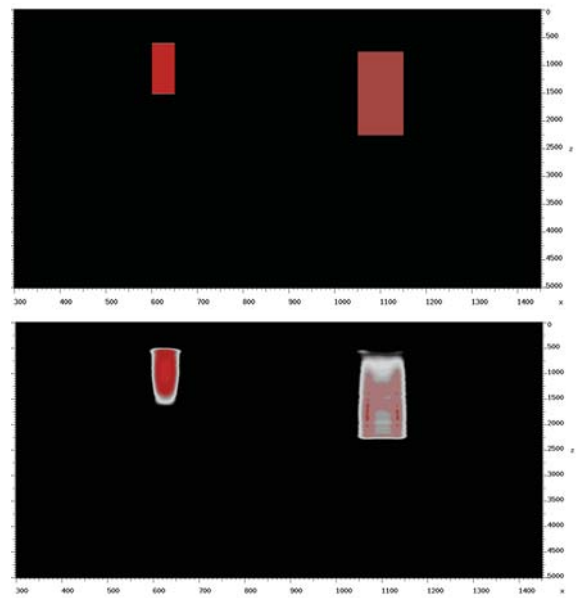

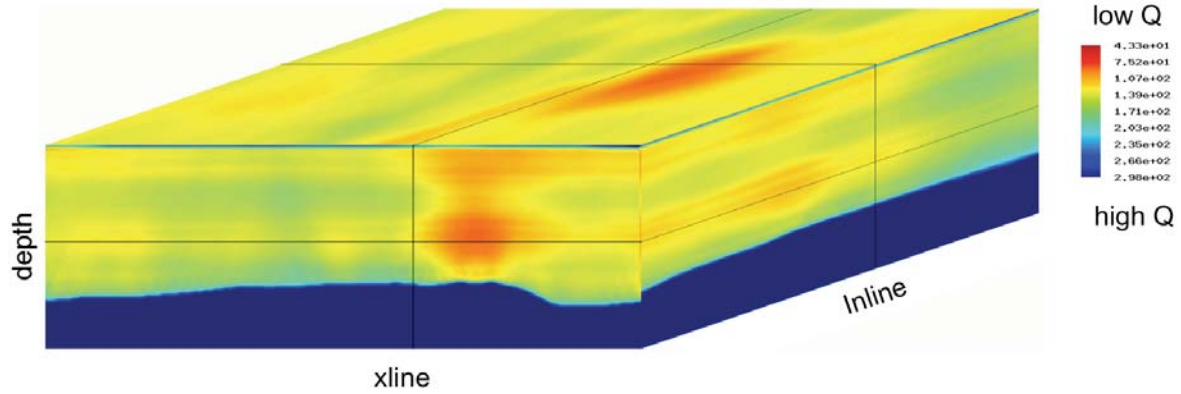*Figure 2* Q models showing two anomalies: Original model (top), tomographic model (bottom).
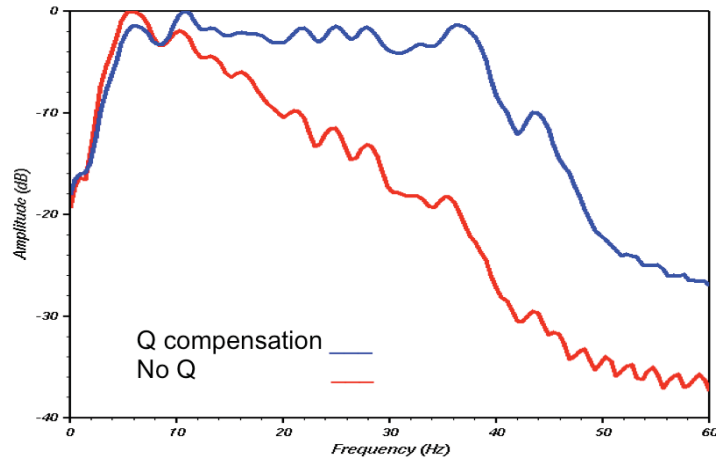

Figure 3 3D tomographic Q model.

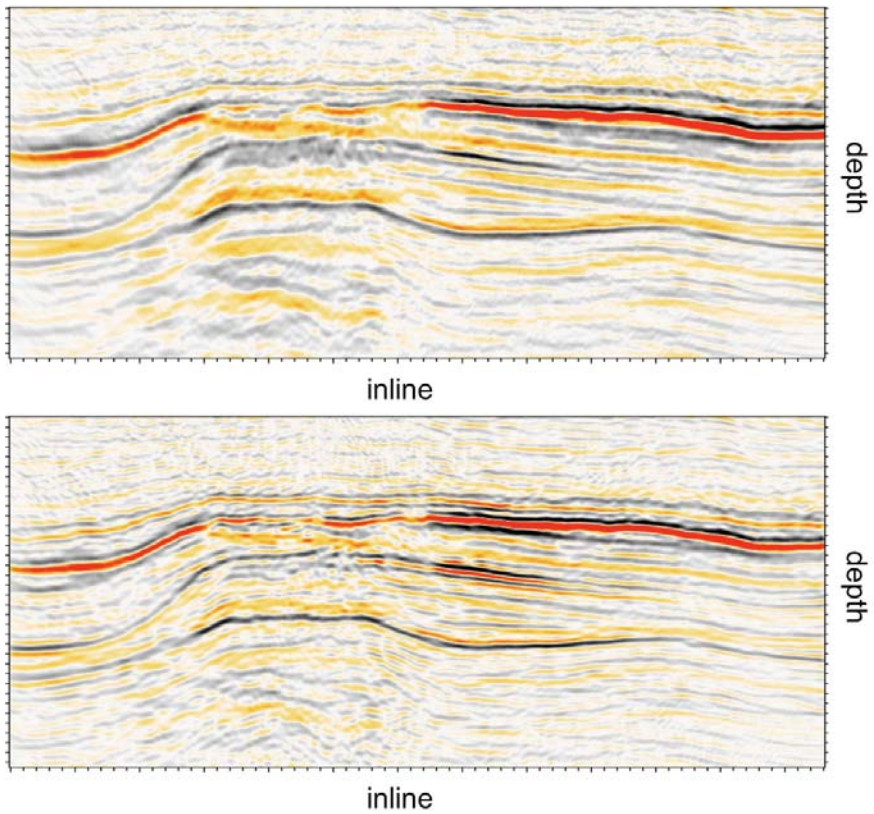*Figure 4* Migrated images spectra comparison after depth to time conversion.

Figure 5 *Migrated images without (top) and with (bottom) Q compensation.*
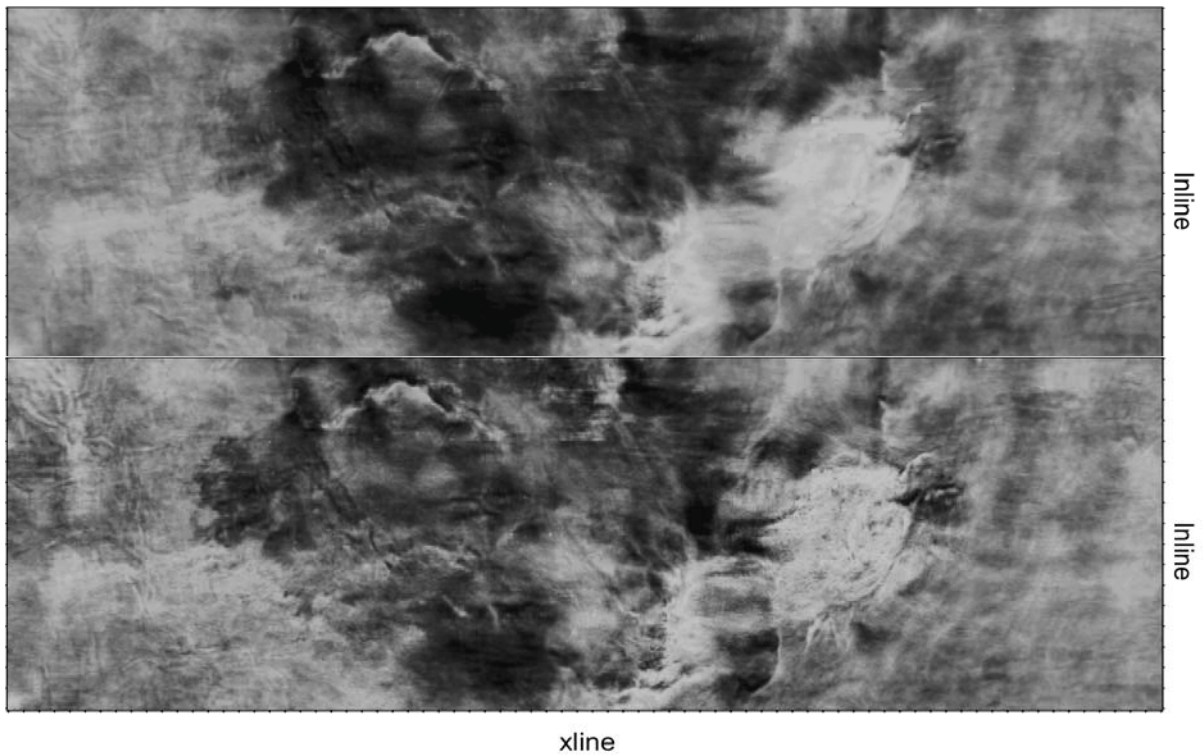

Figure 6 *RMS amplitude attribute on the migrated images without (top) and with (bottom) Q compensation.*